Appl Phys A (2011) 103: 89–96
DOI 10.1007/s00339-011-6305-4

Applied Physics A
Materials Science & Processing

Electrical characterization and fabrication of organic/inorganic semiconductor heterojunctions

B. Boyarbay · H. Çetin · A. Uygun · E. Ayyildiz

Received: 5 October 2010 / Accepted: 10 January 2011 / Published online: 2 February 2011

Abstract Thin films of polyaniline (PANI) titanium dioxide (TiO_2) nanocomposites prepared with and without surfactant (tetradecyltrimethylammonium bromide, TTAB) were formed by spin coating onto chemically cleaned p-type silicon substrates. The current–voltage characteristics of the *Au/PANI TiO_2/p-Si/Al* and *Au/PANI TiO_2 TTAB/p-Si/Al* heterojunctions had rectifying behavior with the potential barrier formed between the polymeric thin films and *p-Si* semiconductor, and they were analyzed on the basis of the standard thermionic emission (TE) theory. Cheung functions combined with conventional forward I–V characteristics were used to obtain diode parameters such as barrier height, ideality factor and series resistance (R_s). The values of barrier height, ideality factor and R_s were found as 0.496 ± 0.003 eV, 2.313 ± 0.067 and 23.633 ± 7.554 Ω for the *Au/PANI TiO_2/p-Si/Al* device; 0.494 ± 0.003 eV, 2.167 ± 0.018 and 12.929 ± 2.217 Ω for the *Au/PANI TiO_2 TTAB/p-Si/Al* device. In addition, the energy distributions of the interface state density of the devices were determined from the forward I–V characteristics by taking into account the bias dependence of the ideality factor and barrier height. It was seen that the *PANI TiO_2 TTAB/p-Si* device had slightly higher interface state density values than those of the *PANI TiO_2/p-Si* device.

Keywords Organic/inorganic semiconductor heterojunctions · Conducting polymers · Thermionic emission · Schottky barrier · Interface states · Series resistance

1 Introduction

Metal/semiconductor (MS) structures have an important role in advanced technology devices [1–5]. The performance and reliability of these structures depend on the properties of the interfaces between metal and semiconductor. An ideal interface is defined by abrupt transition from one material to the next. The equilibration process between two materials is determined by the bulk properties of the constituent materials [5–7]. The MS structure is characterized by its barrier height. The barrier height is equal to the difference between the edge of the respective majority carrier band of the semiconductor and the Fermi level at the interface. On the other hand, the electronic properties of MS structures can be modified by the insertion of an interfacial layer between metal and semiconductor [8–14]. In principle, the introduction of interlayer consisting of conventional semiconductor materials is flexible. But the selection is strongly restricted by the required lattice match between inorganic semiconductor and the interlayer material, resulting in expensive fabrication [1].

In recent years, conjugated polymers have been used as an alternative to conventional inorganic semiconductors in the fabrication of electronic and optoelectronic devices [15, 16]. These devices included field effect transistors (FETs), Schottky diodes, light-emitting diodes (LEDs),

B. Boyarbay · E. Ayyildiz (✉)
Faculty of Science, Department of Physics, Erciyes University, 38039 Kayseri, Turkey
e-mail: enise@erciyes.edu.tr
Fax: +90-352-4374933

H. Çetin
Faculty of Arts and Sciences, Department of Physics, Bozok University, 66100 Yozgat, Turkey

A. Uygun
Faculty of Arts and Sciences, Department of Chemistry, Süleyman Demirel University, 32260 Isparta, Turkey

and so on [15–33]. But the low mobility observed in most of the conjugated polymers is a restrictive factor for device performance, and then undertaking were made on the integration of organic and inorganic semiconductors in hybrid devices having option of allows a simultaneous benefit from the cheaper and more flexible organic materials and processes [28]. Polyaniline (PANI), among various other conducting polymers such as polypyrrole and polyacetylene, has been studied because of its attractive practical properties, e.g. relatively good environmental stability, optimum conductivity and ease of preparation, either chemically or by electrochemical polymerization [28–31]. Although they were widely used in the fabricated of devices, improvement of some electrical and interfacial characteristics such as poor reproducibility is required [26]. Therefore, polymer–inorganic composite materials have also been extensively studied [31–33]. Among these polymers, PANI has attracted considerable attention for the preparation of its composites with inorganic particles to improve their process ability. TiO_2 is known as a *n*-type, while PANI is a *p*-type. Additionally, PANI/TiO_2 based structures have received much attention owing to their high current production in an external circuit by excitons dissociation at the TiO_2 and conjugated polymer interface. These heterojunction structures confirmed high charge separation and charge carrier transport through the metal oxide and the hole-conducting materials, respectively [7, 15, 16]. For efficient conducting polymer/metal oxide based heterojunction structure, an important challenge is preventing the recombination of excitons. The charge separation and charge transfer at the interface heterojunction is an essential factor for determining the performance of heterojunction structure. These factors are mainly related to the morphology, uniformity, and interconnection of both the layers of the heterojunction thin film. Recently, surfactant self-assemblies have been employed as soft-templates to control the size and shape of nanoparticles [34–36]. Surfactant molecules can assemble themselves in ordered structures with particular morphologies in solution because of their hydrophilic and lipophilic properties [37]. This big surface area may be reason of the higher conductivity of the TiO_2/PANI-TTAB composite. It could be concluded that these modifications in the synthesis using surfactant could enhance the performance of the heterojunction structure.

We fabricated polymer-inorganic composite/inorganic semiconductor heterojunctions by using thin films of polyaniline (PANI) titanium dioxide (TiO_2) composites prepared with and without surfactant and *p*-Si. It was seen that the *I*–*V* characteristics of the devices had rectifying behavior with a potential barrier forming between the polymer thin films and *p*-Si semiconductor. The aim of our study was to examine how the presence of surfactant affects the parameters of the junction, such as the ideality factor, barrier height, series resistance and interface state density distribution. For this reason, the *I*–*V* characteristics of the devices were analyzed on the basis of standard thermionic emission (TE) theory.

2 Experimental procedures

In the present study, *p*-type Si wafer with a (100) orientation and a doping density of $\sim 10^{15}$ cm^{-3} was used. The wafer was chemically cleaned using the RCA cleaning procedure (i.e., a 10 min boil in $NH_4+ H_2O_2 + 6H_2O$ followed by a 10 min boil in $HCl + H_2O_2 + 6H_2O$) [38]. Before aluminum (Al) ohmic contact formed on the substrate, the sample was dipped in dilute HF:H_2O (1:10) for about 30 s to remove any native thin oxide layer on the surface, then rinsed with de-ionized water (purity up to 18.2 MΩ cm) and dried with high-purity N_2 gas. The ohmic contact was made by evaporating Al on the back surface of the *p*-Si substrate. The Al plus *p*-Si system was thermally annealed at 570°C for 3 min in N_2 atmosphere to form a heavily doped *p*-type region (*p*+) [6]. Evaporated film thickness was monitored using a quartz oscillator and the metal films had a thickness of 500 Å. The wafer was then cut into two pieces.

The chemical syntheses of the PANI/TiO_2 composites in an aqueous medium with and without cationic tetradecyltrimethylammonium bromide (TTAB) were made following the procedure described elsewhere in the literature [37, 39]. Polyaniline (PANI) titanium dioxide (TiO_2) composites prepared with and without surfactant were characterized by Fourier Transform Infrared (FTIR) and Ultraviolet-visible (UV-visible) spectroscopy. FTIR and (UV-vis) spectra revealed that an interaction existed between the TiO_2/composite and surfactant [37]. The chemically synthesized PANI TiO_2 and PANI TiO_2 TTAB were dissolved in *N*-methyl pyrrolidine (NMP), filtered through a 0.20 µm filter and then used to form thin films by spin coating (50 s at 3500 rpm on a Delta6 RC spin coater) on *p*-Si substrate. The thicknesses of the polymeric films were measured to be 105 nm by a profilometer. Finally, a circular top metal contact with a 550 Å thickness was obtained by gold (Au) evaporation at about 3×10^{-6} mbar pressure by using a shadow mask. Thus, the *Au/PANI TiO_2/p-Si/Al* and *Au/PANI TiO_2 TTAB/p-Si/Al* heterojunctions were fabricated. These samples were called SD1 (first dot of sample with surfactant), SD2 and SD3; D1 (first dot of sample without surfactant), D2 and D3. A schematic device structure of the heterojunction is shown in Fig. 1. The current–voltage (*I*–*V*) characteristics of the devices were performed in the dark and at room temperature, by using an HP 4140B Picoammeter/Voltage Source.

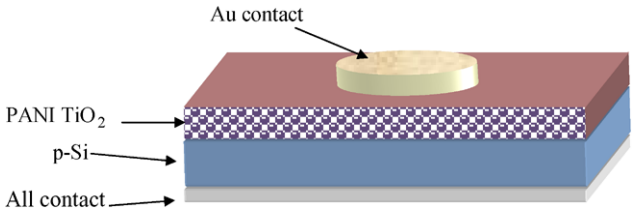

Fig. 1 A schematic device structure of the heterojunctions

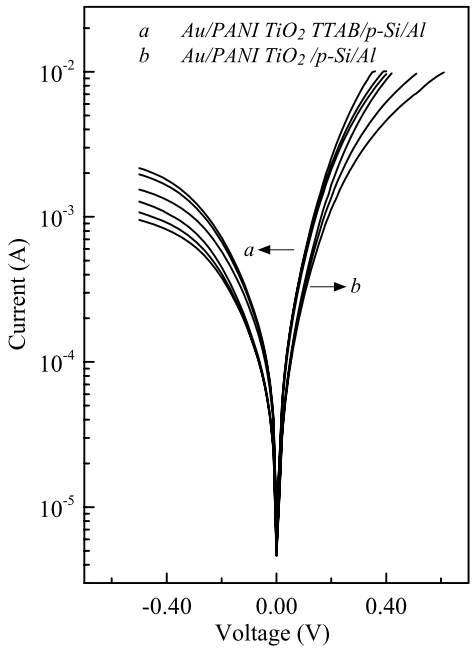

Fig. 2 The experimental semi-log forward and reverse bias I–V characteristics of the *Au/PANI* TiO_2/*p-Si* and Au/*PANI* TiO_2 *TTAB*/*p-Si* heterojunctions, at room temperature. *a* indicates SD1, SD2 and SD3; *b* indicates D1, D2 and D3 diodes

3 Results and discussion

The experimental semi-logarithmic plots of forward and reverse currents versus the applied voltage of the *Au/PANI* TiO_2/*p-Si/Al* and *Au/PANI* TiO_2 *TTAB*/*p-Si/Al* heterojunctions are shown in Fig. 2, at room temperature. In the forward bias, Al was positively biased and Au negatively biased for the *Au/PANI* TiO_2/*p-Si/Al* and *Au/PANI* TiO_2 *TTAB*/*p-Si/Al* heterojunctions. As can be seen from Fig. 2, the I–V characteristics of these heterojunctions exhibit a diode-like behavior. This behavior can be attributed to the formation of a potential barrier between the nanocomposite thin film and *p*-Si substrate. Characteristic diode parameters such as the ideality factor, barrier height and series resistance of devices can be obtained from analysis of these plots.

When the Schottky barrier diode with a series resistance and an interfacial layer is assumed, the current through the diode may be described in terms of the thermionic emission of carriers over a barrier and is given by [5, 6]

$$I = I_0 \exp\left(\frac{q(V - IR_s)}{nkT}\right)\left\{1 - \exp\left(-\frac{q(V - IR_s)}{kT}\right)\right\} \quad (1)$$

where I_0 is the saturation current and is expressed as

$$I_0 = AA^*T^2 \exp\left(-\frac{q\Phi_{b0}}{kT}\right) \quad (2)$$

where A is the effective area of the diode, A^* is the effective Richardson constant and equals 32 $\mathrm{A\,cm^{-2}\,K^{-2}}$ for the *p*-type *Si* semiconductor [6], T is the operational temperature in Kelvin, k is Boltzmann constant of 1.38×10^{-23} $\mathrm{J\,K^{-1}}$, q is the elementary charge, Φ_{b0} is the apparent or effective barrier height obtained from the extrapolation of I_0 in the semi-log forward bias $\ln I$–V characteristics according to [5, 6]

$$q\Phi_{b0} = kT \ln\left(\frac{A^*AT^2}{I_0}\right) \quad (3)$$

and n is the ideality factor. In this equation, n is a dimensionless parameter introduced to account for the departures from thermionic emission theory (ideally $n = 1$). The value of n is calculated from the slope of the linear region of the forward I–V characteristics according to [5, 6]

$$n = \frac{q}{kT}\frac{dV}{d(\ln I)}. \quad (4)$$

The experimental parameters of the *Au/PANI* TiO_2/*p-Si/Al* and *Au/PANI* TiO_2 *TTAB*/*p-Si/Al* heterojunctions are given in Table 1. The values of the ideality factor n of the *Au/PANI* TiO_2/*p-Si/Al* and *Au/PANI* TiO_2 *TTAB*/*p-Si/Al* heterojunctions were obtained from the linear regions of the forward I–V characteristics (Fig. 2) that include the effect of the interfacial parameters rather than that of the series resistance [2, 5]. As can be seen from Table 1, the effective barrier height and ideality factors for the devices varied from diode to diode even if they are identically prepared. Therefore, it is common practice to take averages. When considering all of the heterojunctions, the statistical analysis of the I–V plots yields a mean barrier height value of 0.504 eV with a standard deviation of 10 meV, and the mean ideality factor 1.994 with a standard deviation of 0.037 for the *Au/PANI* TiO_2 *TTAB*/*p-Si/Al* heterojunctions, and a mean barrier height value of 0.521 eV with a standard deviation of 40 meV, the mean ideality factor 1.707 with a standard deviation of 0.161 for the *Au/PANI* TiO_2/*p-Si/Al* heterojunctions. The high values of the ideality factor for both diodes may be attributed to the presence of a native oxide layer and barrier inhomogeneity, which formed between the

Table 1 The values of diode parameters obtained from the forward bias *I–V* characteristics of the *Au/PANI TiO2/p-Si* and *Au/PANI TiO2 TTAB/p-Si* heterojunctions

Diodes	*I–V*		*dV/d* ln *I–I*		*H(I)–I*	
↓	*n*	Φ_b (eV)	*n*	R_s (Ω)	Φ_b (eV)	R_s (Ω)
TD1	2.028	0.502	2.189	13.487	0.491	13.575
TD2	2.012	0.505	2.169	15.324	0.493	15.395
TD3	1.942	0.504	2.143	9.979	0.492	9.976
	1.994 ± 0.037	0.504 ± 0.001	2.167 ± 0.018	12.929 ± 2.217	0.494 ± 0.003	12.982 ± 2.252
D1	1.695	0.527	2.290	14.303	0.493	14.327
D2	1.516	0.531	2.244	23.737	0.495	23.759
D3	1.911	0.521	2.404	32.833	0.499	32.893
	1.707 ± 0.161	0.526 ± 0.004	2.313 ± 0.067	23.633 ± 7.554	0.496 ± 0.003	23.660 ± 7.580

nanocomposite thin film and *p-Si* semiconductor. It is well known that if *Si* surfaces are prepared by the usual polishing and chemical etching, the Si surface is inevitably covered with a thin insulating film of about 10–30 Å thickness depending on the surface preparation method [40]. It was seen that the *Au/PANI TiO2 TTAB/p-Si/Al* heterojunction had slightly better diode characteristics than those of the *Au/PANI TiO2/p-Si/Al* heterojunction, looking at standard deviations of characteristic diode parameters. The discrepancy between the values of standard deviations and variation of characteristic diode parameters may be attributed to differences of the interfacial layer formed between the nanocomposite thin films and *p-Si* semiconductor. It is known from the literature that the barrier height inhomogeneities can occur as a result of inhomogeneities in the interfacial layer composition, non-uniformity of the interfacial charges and interfacial layer thickness. In such cases, the current across the organic/inorganic junction may be greatly influenced by the presence of the energy barrier inhomogeneity. Yavuz and Gök [37] investigated the thermal, electrical and morphological characteristics of *PANI TiO2* conducting composites prepared in the presence of different surfactants. They reported that all composites had different thermal, electrical and morphological characteristics. FTIR, UV-vis, yields, conductivity and SEM results showed that *TTAB* cationic surfactant had the strongest interaction with the composite matrix. The thermal stability of the *PANI TiO2* composite increased in the presence of cationic surfactants. The direct current electrical conductivities for the *PANI TiO2* and *PANI TiO2 TTAB* composite pellets were measured to be 0.41 and 2.27 S/cm by the standard four-probe method, respectively. Moreover, the SEM images of the *PANI TiO2* composite indicated that the *PANI TiO2 TTAB* composite had a bigger surface area than that of *TiO2/PANI*. We speculated that these modifications in the synthesis using surfactant could be responsible for enhancing the performance of the heterojunction structure.

The barrier height values of 0.504 and 0.526 eV that we obtained for the heterojunctions fabricated in this work from the conducting nanocomposites layer prepared with and without surfactant were higher than those achieved with the *Au/p-Si* Schottky barriers, which were obtained in the range of 0.29–0.35 eV [41–43]. This increase in barrier height can be attributed to thin films of *PANI TiO2* composites prepared with and without surfactant modifying the effective barrier height by influencing the space-charge region of the inorganic substrate, as reported in Refs. [12, 44]. Thus, we have demonstrated the possibility of barrier height enhancement with a difference of about 190 meV between the barrier heights of the diodes.

Many attempts to increase or modify the barrier height of Schottky barrier diodes have been performed by forming an interfacial layer between the metal and semiconductor [8–14]. Çakar et al. [12] reported a barrier height value of 0.827 eV with $n = 2.783$ for the *Sn/Rhodamine-101/p-Si/Al* heterostructure. Moreover, another diode was prepared by using an *n-doped Si* wafer with a 200 nm thermally grown oxide layer and polyaniline (PANI) [22]. After pre-patterning gold electrodes over the oxide via standard lithography and lift-off techniques, the substrate was cleaved through the electrodes. Pinto et al. [22] have obtained a barrier height of 0.49 eV and a diode ideality factor of 4 for the hybrid organic/inorganic semiconductor Schottky nanodiode. El-Nahass et al. [23] have been examined the electrical characteristics of *NiPc* thin films deposited on *p-Si* as a heterojunction, where *NiPc* was nickel phthalocyanine. The values of barrier height and ideality factor for the *NiPc/p-Si* heterojunction were found to be 0.45 eV and 1.5, respectively. Furthermore, Poddar and Luo [21] reported an innovate method to generate the prepared *polypyrrole*(*PPy*)*/p-Si* heterojunction. The developed method was simple and did not involve aggressive chemistry in patterning conducting polymers. The values of barrier height and ideality factor for the PPy/p-Si heterojunction were determined to be

0.57 eV and 6.72, respectively. Organic/Inorganic heterojunction diodes were fabricated by employing *p-Si* and thin films of poly-*N*-epoxipropylcarbazole (PEPC) doped with tetracyanoquinodimethane (TCNQ) by Ahmed et al. [24]. They grew PEPC films on *Si* wafer at room temperature under different gravity (g) conditions, and current–voltage characteristics of the grown hybrid structures were evaluated as a function temperature. In addition, they found that all samples were p–p isotype heterojunctions and the junctions fabricated at a high value of g showed rectifying properties as a function of device temperature [24]. Junction properties have often been found to be sensitive to the preparation methods of the sample and/or the surface treatment conditions.

The interface states, interfacial layer and series resistance are responsible for the nonideal behavior of the forward I–V characteristics of the diodes. Another way to determine diode parameters is to use Cheung's functions [45]. From (1), the following functions can be written [45]:

$$V = IR_s + n\Phi_b + n\frac{kT}{q}\ln\left(\frac{I}{AA^*T^2}\right), \tag{5}$$

$$\frac{dV}{d(\ln I)} = n\frac{kT}{q} + IR_s, \tag{6}$$

$$H(I) = V - n\frac{kT}{q}\ln\left(\frac{I}{AA^*T^2}\right), \tag{7}$$

and

$$H(I) = IR_s + n\Phi_b \tag{8}$$

where Φ_b is the barrier height obtained from the data of the downward curvature region in the forward bias I–V characteristics. Equation (6) should give a straight line for the data of the downward curvature region in the forward bias I–V characteristics. Thus, the slope and y-axis intercept of a plot of $dV/d(\ln I)$ vs. I give R_s and nq/kT, respectively. Using the n value determined from (6) and the data of the downward curvature region in the forward bias I–V characteristics in (7), a plot of $H(I)$ vs. I according to (8) also gives a straight line with the y-axis intercept equal to $n\Phi_b$. The slope of this plot also provides a second determination of R_s, which can be used to check the consistency of Cheung's approach [2, 45]. The $dV/d\ln I$ versus I and $H(I)$ versus I plots of one of the *Au/PANI TiO2/p-Si/Al* and one of *Au/PANI TiO2 TTAB/p-Si/Al* heterojunctions are shown in Figs. 3 and 4, respectively. The values of n and R_s were found to be 2.313 ± 0.067 and $23.633 \pm 7.554\ \Omega$ for the *Au/PANI TiO2/p-Si/Al* devices; 2.167 ± 0.018 and $12.929 \pm 2.217\ \Omega$ for the Au/*PANI TiO2 TTAB/p-Si/Al* devices from the intercepts and the slopes of Figs. 3 and 4, respectively. It was clearly seen that the values of n from

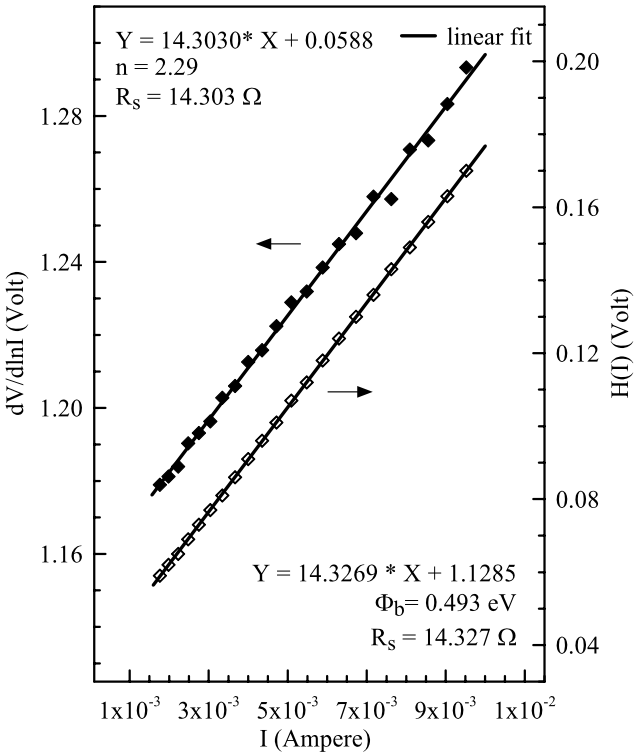

Fig. 3 The experimental $dV/d(\ln I)$ versus I and $H(I)$ versus I plots for one of the *Au/PANI TiO2/p-Si* heterojunctions

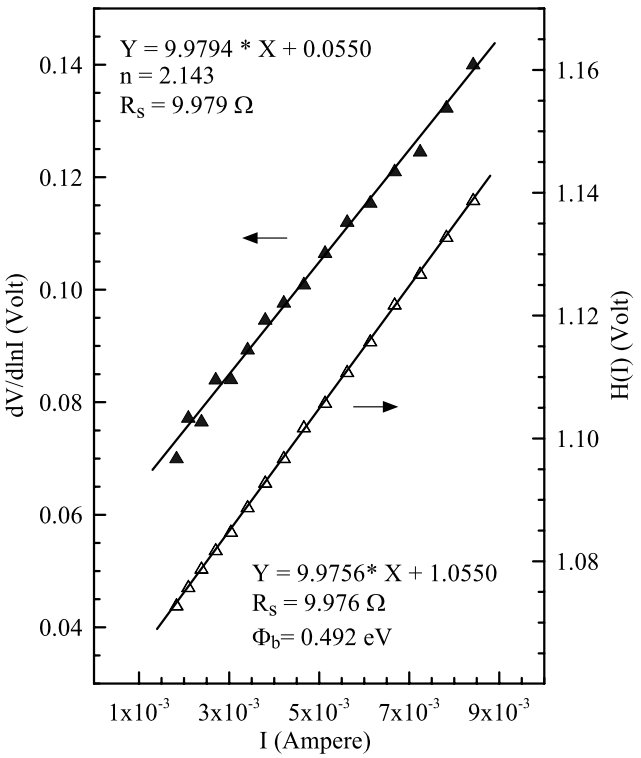

Fig. 4 The experimental $dV/d(\ln I)$ versus I and $H(I)$ versus I plots for one of the *Au/PANI TiO2 TTAB/p-Si* heterojunctions

the downward curvature regions which result from series resistance and interface effects are greater than those obtained from the linear regions of the same characteristics. It is well known that these regions result from the effects of parameters such as interfacial layer thickness, interface state density and the bulk series resistance [45, 46] and to these can also be added the effect of the spatial inhomogeneities of SBHs which are tacitly assumed by all of them [47, 48]. Moreover, barrier height becomes bias-dependent due to the potential change across the interfacial layer thickness as a result of the applied voltage and interface states [1–6, 40]. Thus, the concavity of the current–voltage curve increases at especially high currents in a manner which can be described in terms of an ideality factor n, because the barrier height increases with increasing forward bias voltage. The values of barrier height and R_s were found as 0.496 ± 0.003 eV and $23.660 \pm 7.580\ \Omega$ for the *Au/PANI TiO$_2$/p-Si/Al* devices and 0.494 ± 0.003 eV and $12.982 \pm 2.252\ \Omega$ for the *Au/PANI TiO$_2$ TTAB/p-Si/Al* devices from the intercepts and slopes of Figs. 3 and 4 (H–I plots), respectively. As can be seen from these data, the values of R_s obtained from $dV/d\ln I$–I and $H(I)$–I plots are approximately equal to each other for both diodes. This case shows the consistency of Cheung's approach.

It can be seen that the series resistance for the *Au/PANI TiO$_2$/p-Si/Al* heterojunction is approximately twice that of the *Au/PANI TiO$_2$ TTAB/p-Si/Al* heterojunction. In this case, the thin films of the *PANI TiO$_2$* composite in the presence of surfactant may be more reliable in fabricating diode.

As mentioned in Refs. [7, 49], the interface states and interfacial layer at the organic/inorganic semiconductor heterojunctions play an important role in the determination of the characteristic parameters of the devices. For this reason, the study of interface states is important for the understanding of the electrical properties of such devices. The voltage dependence of the effective barrier height Φ_e under the forward bias condition is contained in the ideality factor n through the relation [40]

$$\frac{d\Phi_e}{dV} = \beta = 1 - \frac{1}{n(V)} \tag{9}$$

where β is the voltage coefficient of Φ_e. That is, for the case when interface states are in equilibrium with the semiconductor and the applied bias dependence of the barrier height β is a parameter which combines effects of both the interface states and interfacial layer thickness. For a sufficiently thick interfacial layer, the relationship between interface states N_{ss} and the ideality factor is given as [6]

$$C_2 = \frac{1}{n} = \frac{\varepsilon_i}{\varepsilon_i + q^2 N_{ss}\delta} \tag{10}$$

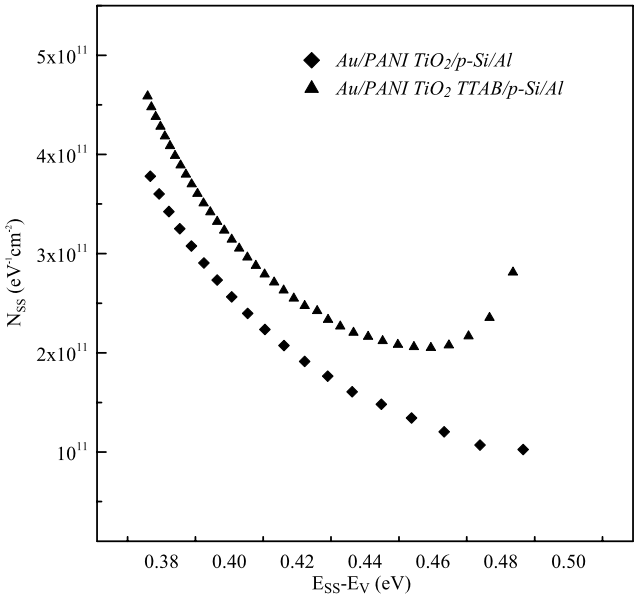

Fig. 5 The energy distribution of interface states for one of the *Au/PANI TiO$_2$/p-Si* and one of the *Au/PANI TiO$_2$ TTAB/p-Si* heterojunctions

where ε_i is the permittivity of the interface oxide layer and δ is its thickness. The average thickness of the oxide layer was measured to be 105 nm by using a profilometer. In this case, the effective barrier height can be written as [40]

$$\Phi_e = \Phi_b + \beta V. \tag{11}$$

The energy of the interface states E_{ss} with respect to the top of the valance band at the surface of the p-type semiconductor is given by [50]

$$E_{ss} - E_v = q\Phi_e - qV. \tag{12}$$

In order to calculate the interface state density distribution for both diodes, substituting the voltage dependence values of n in (10), using $\delta = 105$ nm and $\varepsilon_i = 4\varepsilon_0$, being the permittivity of free space, the values of N_{ss} as a function of V were obtained. These values of N_{ss} were converted to a function of $E_{ss} - E_v$ using (12). The values of the bias dependence of Φ_e in (12) were obtained from (10) and (11). As can be seen from Fig. 5, the exponential growth of the interface state density from midgap toward the top of valance band is very apparent. The interface state density N_{ss} ranges from 1.343×10^{11} eV^{-1} cm^{-2} to 3.513×10^{11} eV^{-1} cm^{-2} for one of the *Au/PANI TiO$_2$/p-Si/Al* devices at the same positions while the *Au/PANI TiO$_2$ TTAB/p-Si/Al* device has interface state density values of 2.059×10^{11} eV^{-1} cm^{-2} at $(0.454 - E_v)$ eV and 4.281×10^{11} eV^{-1} cm^{-2} at $(0.380 - E_v)$ eV. The density distribution curves of the interface states in the range from $(0.380 - E_v)$ eV to $(0.454 - E_v)$

eV are similar to each other. The interface state density values of these two devices are the same order. But these values are lower than that of metal/semiconductor contacts [5, 6].

4 Conclusions

The I–V characteristics of the hybrid organic/inorganic heterojunctions of the *PANI* TiO_2 and *PANI* TiO_2 *TTAB* thin films formed by spin coating onto chemically etched *p-Si* substrate were studied. Surfactant was used to examine how it affects the parameters of junction. It was seen that the I–V characteristics of the fabricated devices displayed rectifying behavior with a barrier height forming between the nanocomposite thin films and inorganic semiconductor. The values of barrier height, ideality factor and R_s were found as 0.496 ± 0.003 eV, 2.313 ± 0.067 and 23.633 ± 7.554 Ω for the *Au/PANI* TiO_2*/p-Si/Al* device; 0.494 ± 0.003 eV, 2.167 ± 0.018 and 12.929 ± 2.217 Ω for the *Au/PANI* TiO_2 *TTAB/p-Si/Al* device. It was seen that these devices had a higher barrier height than that of conventional *Au/p-Si/Al* Schottky barrier diodes that were in the range of 0.29–0.35 eV [41–43]. This increase in barrier height can be attributed to polymeric thin film modifying the effective barrier height by influencing the space-charge region of the inorganic semiconductor *p-Si* substrate [9]. In addition, the energy distributions of the interface states of each device were determined from the forward I–V characteristics by taking into account the bias dependence of the ideality factor and barrier height. It was seen that the interface state densities had an exponential rise with bias from the midgap toward the top of the valance band. The shapes of the density distribution curves of the interface states in the range from $(0.380 - E_v)$ eV to $(0.454 - E_v)$ eV were similar to each other. But the discrepancy between the values of standard deviations and variation of characteristic diode parameters may be attributed to differences of the interfacial layer formed between the nanocomposite thin films and *p-Si* semiconductor. Therefore, the *PANI* TiO_2 TTAB thin film may be used as an active layer between metal and inorganic semiconductor rather than the *PANI* TiO_2.

Acknowledgements This work was supported by the Scientific Research Projects Unit of Erciyes University, Project No EÜBAP-FBA-06-23. The authors would like to thank Erciyes University.

References

1. L.J. Brillson, *Contacts to Semiconductors-Fundamentals and Technology* (Noyes Publications, New Jersey, 1993)
2. E. Ayyildiz, A. Türüt, H. Efeoğlu, S. Tüzemen, M. Sağlam, Y.K. Yoğurtçu, Solid-State Electron. **39**, 83 (1996)
3. R.T. Tung, Mater. Sci. Eng., R Rep. **35**, 1 (2001)
4. H. Çetin, E. Ayyildiz, Semicond. Sci. Technol. **20**, 625 (2005)
5. E.H. Rhoderick, R.H. Williams, *Metal–Semiconductor Contacts* (Clarendon Press, Oxford, 1988)
6. S.M. Sze, K.N. Kwok, *Physics of Semiconductor Devices* (Willey, New York, 2007)
7. M. Lonergan, Annu. Rev. Phys. Chem. **55**, 257 (2004)
8. H. Çetin, B. Şahin, E. Ayyildiz, A. Türüt, Physica B, Condens. Matter **364**, 133 (2005)
9. T.U. Kampen, S. Park, D.R.T. Zahn, Appl. Surf. Sci. **190**, 461 (2002)
10. N. Kavasoglu, C. Tozlu, O. Pakma, A.S. Kavasoglu, S. Ozden, B. Metin, O. Birgi, S. Oktik, Synth. Met. **159**, 1880 (2009)
11. H. Çetin, E. Ayyildiz, A. Türüt, J. Vac. Sci. Technol. B **23**(6), 2436 (2005)
12. M. Çakar, N. Yıldırım, Ş. Karataş, C. Temirci, A. Türüt, J. Appl. Phys. **100**, 074505 (2006)
13. H. Altuntaş, Ş. Altındal, H. Shtrikman, S. Özçelik, Microelectron. Reliab. **49**, 904 (2009)
14. Y.S. Ocak, M. Kulakcı, T. Kılıçoğlu, R. Turan, K. Akkılıç, Synth. Met. **159**, 1603 (2009)
15. W. Brütting (ed.), *Physics of Organic Semiconductors* (Wiley, Weinheim, 2005)
16. N. Koch, Chem. Phys. Chem. **8**, 1438 (2007)
17. F.E. Jones, B.P. Wood, J.A. Myers, C.D. Hafer, M.C. Lonergan, J. Appl. Phys. **86**, 6431 (1999)
18. M. Kaya, H. Çetin, B. Boyarbay, A. Gök, E. Ayyıldız, J. Phys., Condens. Matter. **19**, 406205 (2007)
19. A.S. Riad, Physica B, Condens. Matter. **270**, 148 (1999)
20. L.M. Huang, T.C. Wen, A. Gopalan, Thin Solid Films **473**, 300 (2005)
21. R. Poddar, C. Luo, Solid-State Electron. **50**, 1687 (2006)
22. N.J. Pinto, R. González, A.T. Johnson, A.G. MacDiarmid, Appl. Phys. Lett. **89**, 033505 (2006)
23. M.M. El-Nahass, K.F. Abd-El-Rahman, A.A.M. Farag, A.A.A. Darwish, Org. Electron. **6**, 129 (2005)
24. M.A. Ahmed, Kh.S. Karimovm, S.A. Moiz, IEEE Trans. Electron Devices **51**, 121 (2004)
25. S.R. Forrest, M.L. Kaplan, P.H. Schmidt, J. Appl. Phys. **55**, 1492 (1984)
26. J.M.G. Larajeria, H.J. Khoury, W.M. de Azevedo, E.F. da Silva Jr., E.A. de Vasconcelos, Appl. Surf. Sci. **190**, 390 (2002)
27. I. Musa, W. Eccleston, Thin Solid Films **343**, 469 (1999)
28. W.J. da Silva, I.A. Hümmelgen, R.M.Q. Mello, J. Mater. Sci., Mater. Electron. **20**, 123 (2009)
29. S.F. Chung, T.C. Wen, A. Gopalan, Mater. Sci. Eng. B **116**, 562 (2005)
30. W. Wang, E.A. Schiff, Appl. Phys. Lett. **91**, 133504 (2007)
31. R. Sivakumar, K. Akila, S. Anandan, Curr. Appl. Phys. **10**, 1255 (2010)
32. S.J. Kim, W.J. Kim, A.N. Cartwright, P.N. Prasad, Sol. Energy Mater. Sol. Cells **93**, 657 (2009)
33. S. Güneş, H. Neugebauer, N.S. Sariciftci, Chem. Rev. **107**, 1324 (2007)
34. X. Li, W. Chan, C. Bian, J. He, N. Xu, G. Xue, Appl. Surf. Sci. **217**, 16 (2003)
35. X. Sui, Y. Chu, S. Xing, M. Yu, C. Liu, Colloids Surf. A, Physicochem. Eng. Asp. **251**, 103 (2004)
36. K. Luo, X. Guo, N. Shi, C. Sun, Synth. Met. **151**, 293 (2005)
37. A.G. Yavuz, A. Gök, Synth. Met. **157**, 235 (2007)
38. W. Kern, D.A. Puotinen, RCA Rev. **31**, 187 (1970)
39. A. Gök, B. Sarı, M. Talu, Synth. Met. **142**, 41 (2004)
40. H.C. Card, E.H. Rhoderick, J. Phys. D, Appl. Phys. **4**, 1589 (1971)
41. B.L. Smith, E.H. Rhoderick, Solid-State Electron. **14**, 71 (1971)
42. M.H. Hecht, L.D. Bell, W.J. Kaiser, L.C. Davis, Phys. Rev. B **42**, 7663 (1990)

43. T. Banerjee, E. Haq, M.H. Siekman, J.C. Lodder, R. Jansen, IEEE Trans. Magn. **41**, 2642 (2005)
44. A.R.V. Roberts, D.A. Evans, Appl. Phys. Lett. **86**, 072105 (2005)
45. S.K. Cheung, N.W. Cheung, Appl. Phys. Lett. **49**, 85 (1986)
46. E. Ayyıldız, Ç. Nuhoğlu, A. Türüt, J. Electron. Mater. **31**, 119 (2002)
47. J.H. Werner, H.H. Güttler, J. Appl. Phys. **69**, 1522 (1991)
48. R.T. Tung, Phys. Rev. B **45**, 13509 (1992)
49. K. Potje-Kamloth, Chem. Rev. **108**, 367 (2008)
50. P. Cova, A. Singh, R.A. Masut, J. Appl. Phys. **82**, 5217 (1997)